

Optimal pressure control using switching solenoid valves

Dipl.-Ing. Oussama Alaya

IMI Precision Engineering , Stuttgarter Straße 120, 70736 Stuttgart, E-mail:
oussama.alaya@imi-precision.com

Dr.-Ing. Maik Fiedler

IMI Precision Engineering , Stuttgarter Straße 120, 70736 Stuttgart, E-mail: maik.fiedler@imi-precision.com

Abstract

This paper presents the mathematical modeling and the design of an optimal pressure tracking controller for an often used setup in pneumatic applications. Two pneumatic chambers are connected with a pneumatic tube. The pressure in the second chamber is to be controlled using two switching valves connected to the first chamber and based on the pressure measurement in the first chamber. The optimal control problem is formulated and solved using the MPC framework. The designed controller shows good tracking quality, while fulfilling hard constraints, like maintaining the pressure below a given upper bound.

KEYWORDS: switching valves, model predictive control (MPC), two tank system, transmission line

1. Introduction

A common aim in the most pneumatic applications is to control the pressure in a chamber with constant volume. This is mainly done using a pressure control valve. The pressure control valve and the chamber are connected within a pneumatic line. The influence of the pneumatic tube in the control and stability behavior of such a set-up is still a current research topic and also discussed in [1, 2, 3, 4]. When using two 2/2 switching valves instead of one control valve, the problem has a new setup. It is a system of two coupled pneumatic tanks. The problem has the following formulation: Control flow rate to and from the first tank, in order to control the pressure in the second tank. The measured signal is thereby the pressure in first tank. The aim of this paper is to introduce a control-oriented model for such a pneumatic-setup and to show how optimization-based control frameworks like Model Predictive Control (MPC) can be used for the controller design.

This paper is organized as follows. Section 2 describes two mathematical models of the system. The first one, is a complex model and can't be used for controller design. It is used as a reference model to validate the second one, which is control-oriented. In section 3, the description of the control design and its validation using simulation results are presented followed by a brief summary and outlook.

2. Coupled pneumatic system modeling

The schematic diagram of the pneumatic two-tank system is shown in **Figure 1**. The system consists of two pneumatic chambers connected with a pneumatic tube with length L and inner diameter D . The pressure in the two chambers of volume V_1, V_2 are denoted with p_1, p_2 . The mass flow rates to and from the first chamber (\dot{m}_i, \dot{m}_o) are controlled using two fast switching valves. In addition to the pressure at the tube boundaries, the tube dynamic is characterized by the mass flow rates (\dot{m}_1, \dot{m}_2) from/to the first chamber and to/from the second chamber.

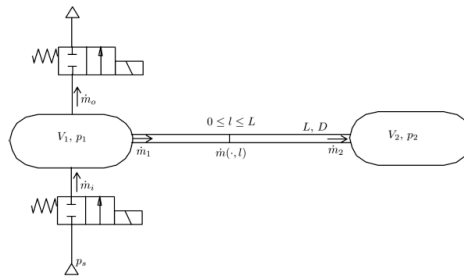


Figure 1: Schematic diagram of the two-tank system

The problem analyzed in this paper can be than formulated as: Control the pressure p_2 based on the measurement of the pressure p_1 using the mass flow rates \dot{m}_i, \dot{m}_o .

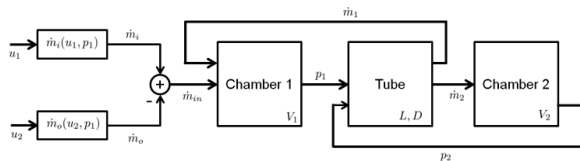


Figure 2: Block diagram of the two-tank system

The whole system consists of the interconnection of the mathematical models of the subsystems (first chamber, second chamber, tube, switching valves). The interconnection is shown in the block diagram in **Figure 2**. The rest of this section deals with the modeling of the subsystems and their combination to the whole system.

2.1. Tube model

2.1.1. Reference model

The tube model is based on the linear resistance compressible model and is given by the following set of partial differential equations (PDE)

$$\frac{\partial p(t, l)}{\partial l} = -\frac{1}{A_t} \frac{\partial \dot{m}(t, l)}{\partial t} - R_t \dot{m}(t, l), \quad \text{for } 0 \leq l \leq L \quad (1a)$$

$$\frac{\partial \dot{m}(t, l)}{\partial l} = -\frac{A_t}{c_s^2} \frac{\partial p(t, l)}{\partial t}, \quad \text{for } 0 \leq l \leq L. \quad (1b)$$

With the boundary conditions:

$$p_1 = p(t, 0), \quad p_2 = p(t, L), \quad \dot{m}_1 = \dot{m}(t, 0), \quad \dot{m}_2 = \dot{m}(t, L). \quad (2)$$

Where: $0 \leq l \leq L$ denotes the axial tube cylinder coordinate, c_s is the air sonic speed, R_t is the tube resistance, under laminar flow conditions and $A_t = \frac{\pi D^2}{4}$ is the cross sectional area of the tube.

For more details about the transmission line modeling, the reader is referred to /1, 2, 4/. The notations used in this paper are adapted from /1/. The exact solution of this partial differential equation is only given in the frequency domain. Unlike the model in /1/, the transmission line model inputs are the pressure at the boundaries (p_1, p_2). Its outputs are the mass flow rates (\dot{m}_1, \dot{m}_2). The frequency domain exact solution for this model is given in /3/ by the following transfer function.

$$\begin{pmatrix} \dot{m}_1(s) \\ \dot{m}_2(s) \end{pmatrix} = G_t(s) \begin{pmatrix} p_1(s) \\ p_2(s) \end{pmatrix} \quad (3)$$

Where the transfer matrix $G_t(s)$ and the frequency dependent coefficients $\Gamma(s)$ and $Z(s)$ are given by:

$$G_t(s) = \begin{pmatrix} \frac{\cosh \Gamma(s)}{Z(s) \sinh \Gamma(s)} & \frac{1}{Z(s) \sinh \Gamma(s)} \\ \frac{1}{Z(s) \sinh \Gamma(s)} & \frac{\cosh \Gamma(s)}{Z(s) \sinh \Gamma(s)} \end{pmatrix}, \quad (4)$$

$$\Gamma(s) = \frac{1}{c_s} \sqrt{(A_t R_t + s)s}, \quad Z(s) = \frac{c_s}{A_t} \sqrt{\frac{(A_t R_t + s)}{s}}. \quad (5)$$

This frequency domain solution is used, like in the literature, as a reference solution. It is not suitable for control design.

2.1.2. Time domain tube model approximation

There are many approaches to approximate this reference model with a control oriented model. One of these approaches is based on the approximations of the frequency domain solutions (3) using its Taylor series (Modal approximations) [1, 3]. The time domain approximation approach is based on the spatial discretization (i.e. the discretization into n-tube segments using some numerical integration method (like forward or backward Euler)) of the PDE (1). In this way the PDE-set (1) is transformed into a set of ordinary differential equations (ODE). Both methods are still current research topic. The approximation used in this paper is the corrected approximation used in [1] and is given as the following ODE-set:

$$\ddot{m}_2 = \frac{A_t}{L} (p_1 - p_2 - R_t L \dot{m}_2) \quad (6a)$$

$$\dot{p}_1 = \frac{\pi^2 c_s^2}{4LA_t} (\dot{m}_1 - \dot{m}_2) \quad (6b)$$

The adaption of the ODE-set (6) for the problem setup shown in the block diagram Figure 2 will be done after formulating the models for the pressure in the two chambers.

2.2. Chamber pressure models

Assuming an isothermal process (T_n constant), the pressure in the first and in the second chambers are given by the following ODEs:

$$\dot{p}_2 = \frac{R_s T_n}{V_2} \dot{m}_2, \quad (7)$$

$$\dot{p}_1 = \frac{R_s T_n}{V_1} (\dot{m}_{in} - \dot{m}_1), \quad (8)$$

where R_s is the air-specific gas constant, $\dot{m}_{in} = \dot{m}_i - \dot{m}_o$ is the combined mass flow rate input from the two switching valves, as shown in Figure 2 .

2.3. Two-tank system model

2.3.1. Reference model

The reference model for the two tank system is constructed by transforming the ODEs (7) and (8) in the frequency domain and connecting them with (4). The Transformation of (7) and (8) into the frequency domain leads to the frequency domain representation.

$$\begin{pmatrix} p_1(s) \\ p_2(s) \end{pmatrix} = \underbrace{\begin{pmatrix} -\frac{R_s T_n}{sV_1} & 0 \\ 0 & \frac{R_s T_n}{V_2} \end{pmatrix}}_{G_c(s)} \begin{pmatrix} \dot{m}_1(s) \\ \dot{m}_2(s) \end{pmatrix} + \underbrace{\begin{pmatrix} \frac{R_s T_n}{sV_1} \\ 0 \end{pmatrix}}_{G_{ci}(s)} \dot{m}_{in}(s) \quad (9)$$

Combining (9) and (3) together leads to the two input to output transfer functions:

$$\begin{pmatrix} p_1(s) \\ p_2(s) \end{pmatrix} = (I - G_{c(s)} G_{t(s)})^{-1} G_{ci}(s) \dot{m}_{in}(s), \quad (10a)$$

$$\begin{pmatrix} \dot{m}_1(s) \\ \dot{m}_2(s) \end{pmatrix} = (I - G_{c(s)} G_{t(s)})^{-1} G_t(s) G_{ci}(s) \dot{m}_{in}(s), \quad (10b)$$

where I is the 2x2 unity matrix. The same result can be obtained using the Redheffer star product framework for interconnecting dynamic systems.

The model (10) is used as a reference model to validate the state space model introduced in the next subsection.

2.3.2. State space model

The Combination of the ODEs (6), (7) and (8) together and the introduction of the following notations:

- the state space vector $x = (x_1, x_2, x_3)^T = (p_1, p_2, \dot{m}_2)^T$, the input $u = \dot{m}_{in}$ and the output vector $y = (y_1, y_2)^T = (p_1, p_2)^T$

lead to the state space model:

$$\dot{x} = \mathbf{A} x + \mathbf{B} u \quad (11a)$$

$$y = \mathbf{C} x + \mathbf{D} u. \quad (11b)$$

Where the system matrices for state space realization (\mathbf{A} , \mathbf{B} , \mathbf{C} , \mathbf{D}) are given as:

- $\mathbf{A} = \begin{pmatrix} 0 & 0 & -a \\ 0 & 0 & \frac{R_s T}{V_2} \\ \frac{A_t}{L} & -\frac{A_t}{L} & -A_t R_t \end{pmatrix}$, where the coefficient a defined as $a = \frac{\pi c_s V_1}{D^2 L V_1 + \pi R_s T_n}$

$$\bullet \quad \mathbf{B} = (a, 0, 0)^T; \quad \mathbf{C} = \begin{pmatrix} 1 & 0 & 0 \\ 0 & 1 & 0 \end{pmatrix}; \quad \mathbf{D} = (0, 0)^T.$$

Some more Model Insights:

By replacing the state variable $x_3 = \dot{m}_2 = \frac{V_2}{R_s T_n} \dot{p}_2$, the dependency of the pressure p_2 on the pressure p_1 becomes clearer. This dependency can be rewritten as a scalar second order system of the form

$$\alpha_2 \ddot{p}_2 + \alpha_1 \dot{p}_2 + \alpha_0 p_2 = \beta p_1. \quad (12)$$

This system representation enables to easily design a dynamic state observer. It is therefore assumed in the rest of this paper that the whole state vector is available for the control base on an observer. Furthermore it is possible to use the presentation to transform the system to a mechanical equivalent system (two mass oscillator) or to an electrical equivalent system (RLC).

The response of the linear system (11) on a mass flow rate truncated step of the amplitude 7g/s, during 60ms (i.e. the input step is truncated after 60ms) is simulated using the following system set up. $D = 4mm$; $L = 2,5m$; $V_1 = 1.5 \text{ cm}^3$; $V_2 = 30V_1$

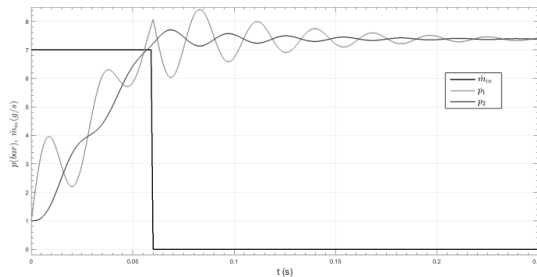


Figure 3: Truncated step response simulation.

As shown in the simulation results in **Figure 3**, the rise time for the pressure signals are at about 40ms and oscillate with a period of about 22ms. It is therefore sufficient, if the linear system frequency response approximate these of the exact system up to a radial frequency of $\omega_r = 2 \pi \frac{1}{22ms} \approx 285 \frac{\text{rad}}{\text{s}}$. The fulfillment of this requirement will be checked in the next subsection.

2.4. Frequency domain model validation

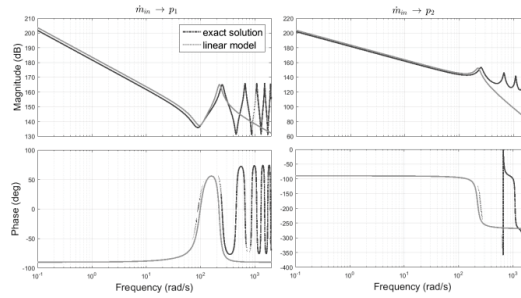


Figure 4: Bode diagram for the transfer functions $\dot{m}_{in} \rightarrow p_1, p_2$

The input-to-output frequency response of the state space model (11) is compared to the frequency response of the reference model (10). The interesting system outputs are the pressure p_1, p_2 in the two chambers which are at the same time the measured output and the performance (to be controlled) output. As shown in **Figure 4**, the linear model is good approximation of the exact model in the frequency band $\left[0.1 \frac{rad}{s}, 300 \frac{rad}{s}\right]$. The requirement of the last subsection is therefore fulfilled and the state space model (11) can be used as control oriented system model.

2.5. Control oriented model for the switching valves

The mass flow rates \dot{m}_i and \dot{m}_o have usually a nonlinear dependency on the pressure p_1 and on the control variables u_1, u_2 . The nonlinear dependency on the control variable can be neglected and assumed to be linear using some feedback-linearization techniques based in model inversion or on Lie derivative (see e.g /5/). The model can be therefore represented as:

$$\dot{m}_i = f_{nl}(u_1, p_1) \approx u_1 \dot{m}_{i_{max}}(p_1); \quad \dot{m}_o = g_{nl}(u_2, p_1) \approx u_2 \dot{m}_{o_{max}}(p_1); \quad u_1, u_2 \in [0, 1] \quad (14)$$

The maximal mass flow rates have a nonlinear dependency on the operating point p_1 . This nonlinear dependency leads to a parameter varying input matrix \mathbf{B} . This is neglected in this paper and will be analyzed in future works using linear parameter varying (LPV) control techniques.

Combining this representation with the state space presentation (11) leads to the 2-Inputs 2-Outputs system

$$\dot{x} = \mathbf{A} x + \mathbf{B}_2 \mathbf{u}; \quad \text{with:} \quad \mathbf{u} = (u_1, u_2)^T; \quad \mathbf{B}_2 = (\mathbf{B} \dot{m}_{i_{max}}, -\mathbf{B} \dot{m}_{o_{max}}) \quad (15a)$$

$$y = \mathbf{C} x + \mathbf{D}_2 \mathbf{u}. \quad \text{with:} \quad \mathbf{D}_2 = (\mathbf{D}, -\mathbf{D}) \quad (15b)$$

The model (15) is used in the next section in order to design an optimal controller based on the Model Predictive Control (MPC) framework.

3. MPC controller design

MPC design is based on formulating the control problem as an optimization problem over a given time horizon and solving it online at each control sample. The optimization problem is solved numerically based on efficient numerical algorithms /6/. The application of MPC in the control of a 4 coupled liquid tanks is analyzed in /7/. MPC algorithms have many advantages like: the ability to considerate of hard input, state constraints, its robustness and the consideration of the system dynamics. On the other side, the main drawback using MPC is its applications in real time. Some of the new results propose explicit MPC (EMPC) algorithms which solve the problem offline based on a polyhedral partition of the state space and a piecewise affine control actions /8/.

3.1. Control problem formulation

The structure of the problem defined in (15) is ready to use for the \mathcal{H}_2 or the \mathcal{H}_∞ frameworks. This will be done in future works. The aim of this paper is the use of the MPC framework. The control problem is therefore first discretized using a sample time t_s . Using the discrete time state space system realization (A_d, B_d, C_d, D_d) of the system (15) and the signal notation $z^k = z(kt_s + t)$, the control problem has the following formulation.

At each time t , for a given desired reference time-varying pressure sequence p_r^k , compute the optimal control sequence $\mathbf{u}^1, \dots, \mathbf{u}^N$ that solves the optimization problem

$$\min_{\mathbf{u}^1, \dots, \mathbf{u}^N} J := \sum_{i=1}^N \|q(y_2^k - p_r^k)\|_p + \|\mathbf{R} \mathbf{u}^k\|_p \quad (16a)$$

$$\text{s. t. : } \begin{cases} \mathbf{x}^k = A_d \mathbf{x}^{k-1} + B_d \mathbf{u}^{k-1}, & \mathbf{y}^k = C_d \mathbf{x}^k + D_d \mathbf{u}^k \\ u_{1k} \in [0,1], u_{2k} \in [0,1] \quad \forall k \in \{1, \dots, N\} & \text{where: } \mathbf{u}_k = (u_{1k}, u_{2k}) \\ y_2 < p_{2max} \end{cases} \quad (16b)$$

Thereby p_{2max} is the maximal allowed pressure in the second chamber and $\|z\|_p$ is the p -norm of the signal z . The matrix \mathbf{R} is a positive definite 2x2 matrix used for weighting the inputs. q is a positive scalar for weighting the output to reference difference $(y_2 - p_r)$. After solving the optimization problem, use the first input \mathbf{u}^1 and then solve the problem (16) at the time $t + t_s$ again.

In order to consider the fact that the control variables u_1, u_2 have a limited change rates, the cost function in (16a) is extended with the term $\mathbf{W} \delta \mathbf{u}^k = \mathbf{W} (\mathbf{u}^k - \mathbf{u}^{k-1})$ which accounts for the change rates in the control variables.

3.2. Closed loop system simulations

For the 1-norm, the problem above is solved using the Multi-Parametric Toolbox 3.0 (MPT3) /8/, using the following numerical parameter values.

$$\mathbf{W} = \begin{pmatrix} 0,1 & 0 \\ 0 & 0,1 \end{pmatrix}, \mathbf{R} = \begin{pmatrix} 1 & 0 \\ 0 & 1 \end{pmatrix}, q = 100, t_s = 10ms, N = 5, \quad p_{2max} = 4.5 \text{ bar}$$

This parameter choice means that the tracking quality is 100 times more important for the cost function than the control inputs and that the control inputs are 10 times more important than their change rates. The problem is discretized with the sample time 10 ms and the optimization problem is solved for the next 5 sample times. In order to make a step ahead in direction of real time MPC for the proposed problem, the MPC controller is transformed to an EMPC controller using the MPT3 Toolbox /8/. The closed loop system is simulated for different output references.

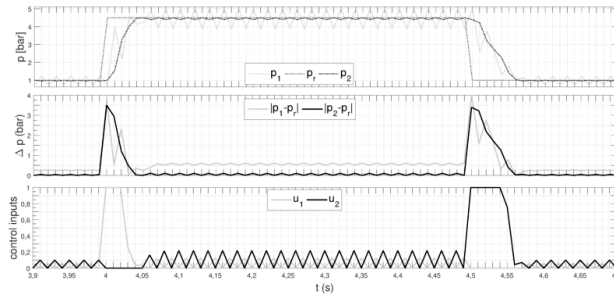


Figure 5: Closed loop step response 1 bar $\rightarrow p_{2max} \rightarrow$ 1 bar

As shown in Figure 5, using the EMPC controller, the system is able to track the reference trajectory with a very good control quality (control error becomes below 0.1 bar within 80ms). Looking at the system behavior near the desired pressure of 1bar, the pressure p_2 is nearly constant =1 bar, while the pressure p_1 has significant oscillations. The transmission of these oscillations is actively damped using the 2 control inputs. The system behavior near the desired pressure of $p_{2max} = 4.5 \text{ bar}$ is a little bit different: The hard constraints on p_2 is fulfilled, while the tracking error in the steady state Δ is lower than 0.15 bar. The fulfillment of the hard constraints means, that the controller is also able to replace a pressure regulator at the cost of more control energy. Furthermore the transmission of the pressure oscillations in the first chamber to the second one is actively damped.

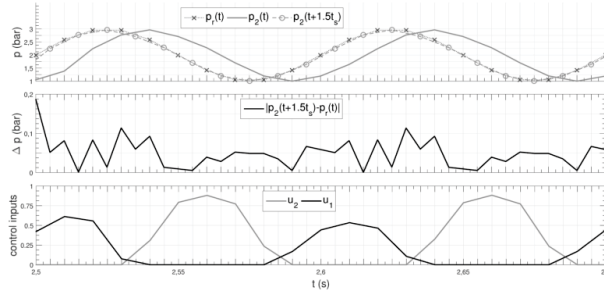


Figure 6: Closed loop sine tracking

Figure 6 shows the simulation results for the tracking of a sine reference pressure with the frequency 10Hz. The tracking quality can be evaluated based on the time delay and on the control error between the time delayed-reference signal and the controlled signal. The time delay of the closed loop system is at about $1.5t_s = 15ms$, while the tracking error is less than 0.1 bar. Unlike classical controller, the MPC controller uses a preview of the reference signal and is able to consider the input and state constraints.

3.3. Explicit MPC controller

Transforming the MPC controller to the explicit form is based on the optimal partition of the augmented state space Ω defined in (17) to m convex subsets $\mathcal{R}_i, i = 1, \dots, m$.

$$\Omega := \{(x|p_r) := (x_1, x_2, x_3, p_r) = (p_1, p_2, \dot{m}_2, p_r) \mid x_{j_{\min}} \leq x_{j=1,2,3} \leq x_{j_{\max}}; p_{r_{\min}} \leq p_r \leq p_{r_{\max}}\} \quad (17)$$

The control input vector \mathbf{u} can be computed online as a piecewise affine function (18) after locating the region \mathcal{R}_i , containing the point $(x|p_r)$.

$$\mathbf{u} = f(x|p_r) = F_i(x|p_r)^T + g_i, \quad \text{for } (x|p_r) \in \mathcal{R}_i, \quad i = 1, \dots, m \quad (18)$$

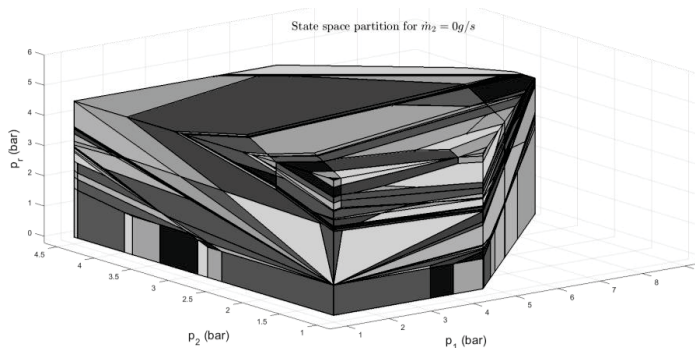


Figure 7: Augmented State space partition for $\dot{m}_2 = 0$

The computation of the regions \mathcal{R}_i and of the parameters F_i, g_i is done offline. The obtained regions for the special case $x_3 = \dot{m}_2 = 0$, which means that the system is in

the steady state, are shown in **Figure 7**. This representation is obtained by slicing the original state space 4D-Partition at $x_3 = \dot{m}_2 = 0$.

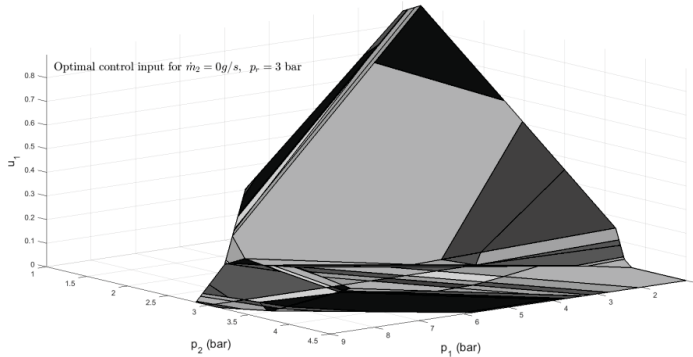


Figure 8: Optimal control inputs

The first control input u_1 (the first component of (18)) is a piecewise map from \mathbb{R}^4 to $[0,1]$. **Figure 8** shows the curve for this map for the reference pressure $p_4 = 3 \text{ bar}$ and starting from a steady state point ($\dot{m}_2 = 0$).

4. Summary and Outlook

This paper presented two state of the art models for a common used pneumatic set up using switching valves. The first model is based on the exact dynamic of the transmission tube and is used as a reference model. The second model has a state space presentation and is validated using the first one and is therefore control-oriented. Based on this model an EMPC controller was designed and validated. The simulations results showed that this framework is very suitable for this applications problem: The EMPC controller has a very good tracking performance. Furthermore, the transmission of the pressure oscillations is actively damped.

Future works will focus in the consideration of the parameter dependency using the LPV framework, on reducing the complexity of the EMPC controller and on experimental validation of the presented controller.

5. References

- /1/ D. Rager, R. Neumann and H. Murrenhoff. Simplified Fluid Transmission Line Model for Pneumatic Control Applications, Proceedings of the 14th Scand. International Conference on Fluid Power, SICFP15, Tampere, Finland, 2015.
- /2/ J. Stecki and D. Davis. 1986. "Fluid transmission lines—distributed parameter models part 1: A review of the state of the art". Proceedings of the Institution

- of Mechanical Engineers, Part A: Journal of Power and Energy 200.4, pp. 215–228.
- /3/ B. Ayalew, B.T. Kulakowsk, Modal Approximation of Distributed Dynamics for a Hydraulic Transmission Line with Pressure Input-Flow Rate Output Causality, Journal of Dynamic Systems, Measurement and Control 127, 503, 2005.
- /4/ J. Kefer, S.V. Kirchel and O. Sawodny, Modeling and Simulation of Pneumatic Systems with Focus on Tubes, IFK 2012, Dresden, 2012
- /5/ H.K. Khalil, Nonlinear Systems. 3. ed. Upper Saddle River, NJ: Prentice Hall, 2002.
- /6/ Camacho, Eduardo F., and Carlos Bordons Alba. Model predictive control. Springer Science & Business Media, 2013.
- /7/ E.P. Gatzke, E.S. Meadows, C. Wang and F. J. Doyle, Model Based Control of a Four-Tank System, Computers & Chemical Engineering 24, no. 2 (2000): 1503–9.
- /8/ M. Herceg, M. Kvasnica, C.N. Jones, and M. Morari. Multi-Parametric Toolbox 3.0. In Proc. of the European Control Conference, pages 502–510, Zurich, Switzerland, July 17–19 2013
- /9/ P. Bigras, PASCAL, T. Wong and R. Botez, Pressure Tracking Control of a Double Restriction Pneumatic System, ASME J. Dynamic Systems, Measurement and Control 128 (2001): 384–90.

6. Nomenclature

L, D, A_t	Tube length, diameter, cross sectional area	m, m, m^2
p_j, V_j	Air pressure in/ and volume of chamber j	Pa, m^3
\dot{m}_*	Mass flow rates	$kg \cdot s^{-1}$
$G_*(s)$	Transfer matrices in the frequency domain	----
$c_s; R_s$	Air sonic speed, Air specific gas constant	$m \cdot s^{-1}; J kg^{-1} K^{-1}$
T_n	Ambient temperature	K